




Article

Lacustrine Wetlands Landscape Simulation and Multi-Scenario Prediction Based on the Patch-Generating Land-Use Simulation Model: A Case Study on Shengjin Lake Reserve, China

Zonghong Zheng ¹, Jie Wang ^{1,2,3,*} , Jianhua Ni ^{1,3} , Yuhuan Cui ⁴  and Qiang Zhu ¹

¹ College of Resources and Environmental Engineering, Anhui University, Hefei 230601, China; x22201015@stu.ahu.edu.cn (Z.Z.); neejianhua@126.com (J.N.); qiangzhuu@163.com (Q.Z.)

² Anhui Province Key Laboratory of Wetland Ecosystem Protection and Restoration, Anhui University, Hefei 230601, China

³ Engineering Center for Geographic Information of Anhui Province, Anhui University, Hefei 230601, China

⁴ College of Resources and Environment, Anhui Agricultural University, Hefei 230036, China; cuiyh@ahau.edu.cn

* Correspondence: wangjie@ahu.edu.cn

Abstract: Landscape simulation and prediction are crucial for understanding the dynamic evolution and future trends of wetlands. However, only a few existing studies have focused on the applicability and limitations of commonly used land-use/cover change (LUCC) simulation models in lake wetland landscapes. Taking Shengjin Lake Reserve in China as the study area, we firstly analyzed landscape variations during 2010–2020 using multisource remote sensing images. Then, the patch-generating land-use simulation (PLUS) model was employed to simulate wetland landscapes in 2020, the accuracy and limitation of which in simulating lacustrine wetlands were also explored. Lastly, the changing trends of wetland landscapes in 2030 under different development scenarios were predicted. The results show that the landscape of Shengjin Lake Reserve has changed significantly during 2010–2020, with increases in mudflats, reservoirs/ponds, woodlands, and built-up land, and there has been decreases in lakes, grass beaches, and croplands. The PLUS model demonstrated an ideal simulation accuracy for Shengjin Lake Reserve, with the overall accuracy exceeding 80%, kappa coefficient greater than 0.75, and figure of merit (FOM) coefficient of 0.35, indicating that the model can capture the dynamic changes in wetland landscapes accurately. The simulation accuracy can be effectively improved with the adjacent initial year, shorter time interval, and the primary driver factors. Under the natural development scenario, the number of patches in the Shengjin Lake Reserve increased sharply, and landscape fragmentation intensified. Under the urban development scenario, the expansion of built-up land increased, and the average patch area increased. In the ecological protection scenario, the Shannon diversity index and Shannon evenness index of the landscape improved significantly, and the natural wetlands such as grass beaches and lakes can be protected effectively. Our study confirms the applicability of the PLUS model in simulating and predicting lacustrine wetlands landscapes, and the conclusions provide a scientific basis for formulating reasonable development strategies to realize wetland resource conservation and management.

Keywords: lacustrine wetlands; PLUS model; multi-scenario simulation; landscape pattern; driving force



Citation: Zheng, Z.; Wang, J.; Ni, J.; Cui, Y.; Zhu, Q. Lacustrine Wetlands Landscape Simulation and Multi-Scenario Prediction Based on the Patch-Generating Land-Use Simulation Model: A Case Study on Shengjin Lake Reserve, China. *Remote Sens.* **2024**, *16*, 4169. <https://doi.org/10.3390/rs16224169>

Academic Editors: Junshi Xia, Dar Roberts, Heidi Van Deventer and Simona Niculescu

Received: 4 October 2024

Revised: 4 November 2024

Accepted: 6 November 2024

Published: 8 November 2024



Copyright: © 2024 by the authors. Licensee MDPI, Basel, Switzerland. This article is an open access article distributed under the terms and conditions of the Creative Commons Attribution (CC BY) license (<https://creativecommons.org/licenses/by/4.0/>).

1. Introduction

Wetland, situated in the transition zone between terrestrial and aquatic ecosystems, is one of the most crucial ecosystems on Earth [1]. With extremely high ecological value and the ability to provide a variety of ecosystem services, wetland is crucial to maintaining biodiversity, ecological security, and human life [2]. Lacustrine wetlands, influenced by

periodic changes in the hydrological environment, form complex and diverse landscapes that play an indispensable role in providing migratory bird habitats, climate regulation, and carbon storage [3,4]. Therefore, exploring the evolution characteristics of lacustrine wetlands landscapes and predicting future trends are of great scientific significance for understanding wetland ecosystems and protecting wetland resources effectively.

The study of wetland landscape pattern evolution can reveal the dynamic changes in wetland ecosystems, which usually adopts methods such as landscape pattern indices and landscape dynamic change models [5,6]. Landscape pattern indices are often used to quantitatively reflect landscape structure and spatial configuration. For example, the Shannon diversity index can be used to describe the diversity of different landscape types within the wetland reserve. However, this method may not be adequate to describe the spatiotemporal dynamics in landscapes. In this case, landscape dynamic change models are needed to better capture the characteristics of the continuous spatial–temporal evolution of landscape patterns. These dynamic models have been widely used to analyze the spatiotemporal evolution of landscape patterns and their driving mechanisms [7,8]. The core of landscape dynamic change models lies in land-use/cover change. Through the analysis, simulation, and prediction of the trend of land-use change, the evolution characteristics of a landscape pattern and its driving mechanism can be explored in depth [9].

The commonly used surface landscape simulation models include the CA–Markov model [10], CLUE-S model [11], ANN model [12], FLUS model [13], and GeoSOS model [14]. However, these models have limitations in terms of simultaneously predicting landscape type, number, and spatial distribution [15–17]. The patch-generating land-use simulation (PLUS) model is a geospatial cellular automata (CA) model based on raster data [18]. It integrates a new land expansion analysis strategy (LEAS) with the CA model based on multiple random patch seeds (CARS), enabling the identification of driving factors for various types of land expansion and the spatiotemporal dynamic simulation of patch-level evolution in multiple land-use landscapes [19]. Scholars have employed the PLUS model to carry out surface landscape simulations at various spatial scales, including in provincial and higher regions [20], urban groups [21], watersheds [22], and coastal areas [23]. In the analysis of the driving force of landscape evolution, existing research mainly relies on principal component analysis, multivariate logistic regression, and CA models [24–26]. However, these models have limitations in terms of extracting transformation rules [27]. For example, transformation analysis strategies (TASs) rely on two-period land-use transition matrices, increasing the complexity for multi-category landscape models [28], while pattern analysis strategies (PASs) use single-period data but lack a temporal dimension and control over driving factors [13]. Additionally, traditional CA models primarily focus on urban expansion, neglecting the dynamic changes in natural landscape patches and the multi-level diversity of ecosystems [29]. The PLUS model effectively addresses these limitations, which can quantitatively analyze the driving forces that cause landscape pattern changes, analyze the contribution rates of various driving factors [30], and quantitatively determine the impact of each factor on landscape changes. Additionally, this model combines landscape simulation models with landscape indices [31], which can quantitatively analyze and describe land-use change and landscape pattern change and has great potential in the simulation and prediction of lacustrine wetlands landscapes. However, due to the strong spatial heterogeneity of landscapes in lacustrine wetlands, the applicability of the PLUS model to simulate the lacustrine wetlands landscape and the limiting factors of its simulation accuracy are not clear.

Shengjin Lake Reserve is one of the lacustrine wetlands in the Yangtze River Basin of China. It was established as a national nature reserve in 1997, joined the network for wetland protection in the middle and lower reaches of Yangtze River in 2007, and was listed in the list of international important wetlands in 2015 [32,33]. The reserve plays a crucial role in ecosystem services and has a significant impact on biodiversity conservation in the middle and lower reaches of the Yangtze River. However, due to the increased intensity of human activity, such as reclaiming land from lakes and netted aquaculture

since the end of the last century [34,35], the reserve faces numerous pressures, such as habitat degradation and landscape fragmentation. Scholars have conducted studies on land-use [36], landscape pattern [37], and ecological risk [38] in the Shengjin Lake Reserve, yet there is a lack of exploration of future landscape development trends. To meet the needs of wetland resource conservation and management in Shengjin Lake Reserve, it is essential to explore the dynamic evolution trend and multi-scenario evolution prediction of the reserve landscape.

We initially conducted dynamic monitoring of the landscape patterns in the Shengjin Lake Reserve from 2010 to 2020, combining multi-temporal remote sensing monitoring with landscape pattern analysis. Subsequently, the PLUS model simulated the reserve landscape in 2020 and quantified the contributions of various driving factors to the evolution of wetland landscapes. Then, we evaluated the accuracy of the landscape simulation results using remote sensing images of the reserve in 2020 to explore the model's applicability and influencing factors. Finally, under three development scenarios of natural development, urban development, and ecological protection, the PLUS model was used to predict the landscape distribution in 2030, and the future evolutionary trends were analyzed. Our study can provide a scientific basis for wetland protection and management decisions in Shengjin Lake Reserve and also provide an effective method for landscape simulation prediction of other lacustrine wetlands.

2. Materials and Methods

2.1. Study Area

Shengjin Lake Reserve (116°55'E to 117°15'E, 30°15'N to 30°30'N) is located in Chizhou city, southern Anhui Province, adjacent to the Yangtze River, covering an area of approximately 333 km² (Figure 1). It has a subtropical monsoon climate dominated by agriculture [32] and supplemented by forestry, which has led to rich wetland resources. The reserve is a seasonal freshwater wetland centered on a shallow lake with a water depth of between 3 and 4 m, which has a wet period from July to September and a drought period from October to December. During the drought period, the decrease in lake water levels exposes large areas of mudflats and grass flats, providing food resources for overwintering migratory birds [38]. As the population around the reserve has increased, human activities such as enclosing lakes for agriculture, netted aquaculture, and urban construction have intensified [33], severely disrupting the ecological balance of the wetland and exacerbating the vulnerability of the ecosystem. The management department of the reserve has implemented a series of ecological restoration measures since 2017, such as establishing ecological red lines, removing lake fences, converting cropland back to wetland, prohibiting fishing, and reverting shores to woodland to safeguard the wetland resources and ecological services of the reserve effectively.

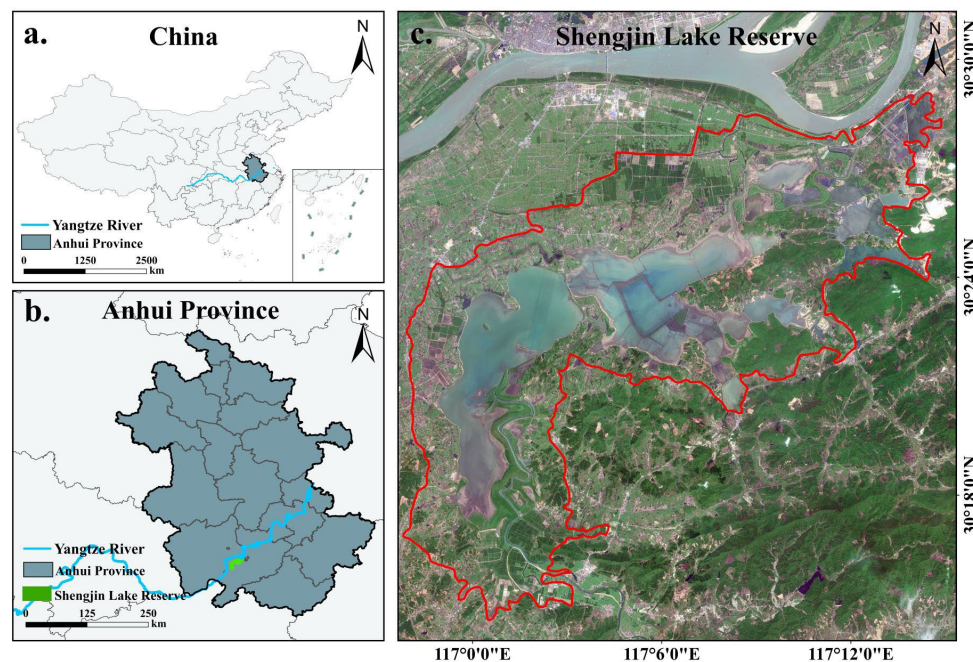


Figure 1. Location of the study area. (a) China; (b) Anhui Province; (c) Shengjin Lake Reserve.

2.2. Data Sources and Preprocessing

2.2.1. Wetland Landscape

According to a field survey of the landscape of Shengjin Lake Reserve in December 2021, we categorized the landscape types into two major classes: wetlands and nonwetlands. Utilizing the wetland classification standard (GB/T 21010-2017) [39] along with related classification studies [40,41], we subdivided the landscape types within the reserve into seven types, namely lakes, mudflats, grass beach, cropland, built-up land, woodland, and reservoirs/ponds (Table 1), and established their remote sensing interpretation indicators. In the classification process, we adopted an object-oriented classification approach, utilizing not only spectral characteristics but also incorporating spatial morphology and texture features to enhance classification accuracy. Additionally, we have referenced land cover features and spatial distribution information to assist in the judgment and validation of the classification results. For example, we distinguished lakes from reservoirs/ponds by analyzing morphological characteristics and evidence of human intervention. Namely, lakes typically have irregular, natural boundaries, whereas reservoirs/ponds tend to have more regular boundaries and are often connected to irrigation facilities or farmland. Seasonal vegetation changes, land-use types, and hydrological characteristics were also used to assist in identifying cropland, mudflats, and grass beaches.

Table 1. The definitions of seven landscape types for the reserve.

Type	Definition
Lakes	Lakes have large water surfaces and relatively stable water levels.
Cropland	Land for agricultural production, including dry land and paddy fields.
Built-up land	Including residential areas, roads, and other artificially developed land.
Mudflats	The intertidal zone at the edge of lakes or rivers is mainly composed of sediment, which is periodically submerged or exposed.
Grass beach	Wetland grasslands covered by vegetation, located around lakes or coastal areas, have the characteristic of periodic inundation.
Woodland	Natural forests and artificial forests, referring to land with tree growth, high coverage, and clear boundaries.
Reservoirs/ponds	A polygonal water body constructed by humans for irrigation, fishing, or other purposes and managed by humans.

At an annual interval of 5 years, remote sensing images captured during the dry season from 2010 to 2020 were selected for landscape classification. The data used included Landsat 7/8 and Sentinel-2 images (Table 2). In this study, we first used ENVI 5.6 and SNAP 8.0 software to mosaic, radiometrically calibrate, and atmospherically correct the remote sensing images. Then, using eCognition 9.0 software, we performed object-oriented multi-scale segmentation (scale 40, shape 0.2, and compactness 0.4) and applied the nearest neighbor image feature algorithm as the specific classification method. This object-oriented classification approach not only utilizes spectral features but also incorporates spatial morphology and texture features, making the classification more precise and effective, particularly for medium- to high-resolution images. The nearest neighbor image feature algorithm, as a simple yet efficient machine learning-based classification method, is especially suitable for handling heterogeneous landscape distributions, such as those found in the Shengjin Lake Reserve. This algorithm can process multidimensional data, making it highly useful for classifying combined spectral band features. Moreover, the nearest neighbor algorithm does not require assumptions about data distribution, allowing it to effectively classify uneven or non-normally distributed data. During classification, the algorithm finds the closest match by comparing the feature vectors of pixels with those of training samples. For feature selection, we used the mean and standard deviation of the red, green, blue, and near-infrared bands as feature vectors, along with spatial morphology and texture features. This combination captures the spectral and spatial characteristics of different land cover types, providing rich information for classification.

Table 2. Datasets used in this study.

Data Type	Data Name	Resolution	Data Sources
Remote sensing images	Landsat7 (2010, 2015)	30 m	http://www.gscloud.cn/ (accessed on 12 November 2022)
	Sentinel-2 (2016, 2020)	10 m	https://dataspace.copernicus.eu/ (accessed on 10 November 2022)
Natural factors	DEM	90 m	http://www.gscloud.cn/ Extracted based on DEM (accessed on 13 May 2023)
	Slope	90 m	
	Temperature	1000 m	https://www.resdc.cn/ (accessed on 20 May 2023)
	Precipitation	1000 m	
Socio-economic factors	Population	1000 m	https://www.resdc.cn/ (accessed on 20 May 2023)
	GDP	1000 m	
	Distance from town	300 m	https://www.webmap.cn/ (accessed on 15 May 2023)
	Distance from road	300 m	

During the classification process, the automated classification results can still be influenced by factors such as sensor resolution, lighting conditions, and atmospheric environment, leading to confusion or misclassification of certain landscape types. Therefore, during field surveys, we collected sample data from different landscape types and compared them with corresponding high-resolution remote sensing images. Through visual interpretation, misclassified areas were manually corrected. For example, some mudflats or grasslands may have been mistakenly classified as water bodies or croplands in the automated classification, and we manually adjusted these areas based on field observation data and high-resolution imagery. In this study, we surveyed a total of 150 field plots, stratified by the seven landscape types within the reserve to ensure full representation of each type. These plots were evenly distributed across different areas of the reserve, covering the seven main landscape types (lakes, mudflats, grass beach, cropland, built-up land, woodland,

reservoirs/ponds). We ensured that each landscape type had at least 20 sample plots to provide sufficient data for classification corrections and accuracy assessment. The final kappa coefficient exceeded 90%.

2.2.2. Driving Factors

Considering the impact of natural factors and human activities on the reserve landscape, eight driving factors were chosen in this paper (Table 2). The digital elevation model (DEM) was from the geospatial data cloud website (<http://www.gscloud.cn>, accessed on 13 May 2023), and the slope was extracted. The annual average temperature, precipitation, gross domestic product (GDP), and population density data were from the Chinese Academy of Sciences Resource and Environmental Science Data Center (<http://www.resdc.cn>, accessed on 20 May 2023); the road and village data were from the National Geographic Information Resources Catalog Service System (<http://www.webmap.cn>, accessed on 15 May 2023), with the distances calculated using the Euclidean distance method. Natural factors such as elevation, slope, temperature, and precipitation reflect the original characteristics of a wetland landscape and its changing trends, while GDP, population density, and distances from roads and towns reflect the disturbance of human activities on the landscape. This selection provides a comprehensive assessment of the wetland landscape evolution process and offers a reliable basis for future landscape pattern predictions. We adjusted the spatial resolution of remote sensing images by resampling it to 15 m to ensure their consistency. For the coarse-resolution data (such as temperature and precipitation), bilinear interpolation methods were applied to match these data to a resolution of 300 m smoothly.

2.3. Methods

2.3.1. Landscape Pattern Analysis

Landscape metrics are widely used to quantitatively express landscape pattern characteristics, providing a comprehensive reflection of landscape structural composition and spatial configuration [42]. We utilized landscape area and proportion to analyze changes in the area and percentage of various landscape types. At both the type and landscape levels, nine landscape metrics were selected [43,44], including shape (largest patch index, LPI; landscape shape index, LSI), fragmentation (number of patches, NP; patch density, PD; and mean patch size, MPS), contagion (contagion index, CONTAG; landscape division index, DIVISION), and diversity (Shannon diversity index, SHDI; Shannon evenness index, SHEI), to describe the landscape pattern of lacustrine wetlands (Table 3). We converted the landscape type images for different years into raster format and used Fragstats 4.2 to calculate the landscape metrics.

Table 3. Landscape pattern indices and their ecological significance.

Index Name	Level	Unit	Ecological Significance
Largest patch index (LPI)	C/L	%	Dominant landscape type and level of human disturbance
Mean patch size (MPS)	C/L	ha	Degree of contagion or division of each patch type in the landscape
Landscape shape index (LSI)	C/L	/	Reflecting the overall complexity of landscape shape
Patch density (PD)	C/L	/	Indicating patch fragmentation and spatial heterogeneity in the landscape
Number of patches (NP)	C/L	/	Complexity of the landscape spatial structure
Landscape division index (DIVISION)	C/L	%	Reflecting the dispersion degree of landscape types
Contagion index (CONTAG)	L	%	Reflecting the connectivity of the landscape
Shannon's diversity index (SHDI)	L	/	Abundance of landscape
Shannon's evenness index (SHEI)	L	/	Proportion of landscape affected by the dominant patch type

Note: C represents the class-level index; L represents the landscape-level index.

2.3.2. PLUS Model

The PLUS model is built on the foundation of cellular automata [18] and includes a quantity prediction module and a spatial distribution simulation module. The former uses existing land-use data with a Markov model to forecast the area of land types in the future, while the latter first utilizes the land expansion analysis strategy to determine the probability of development for each land type [30] and then employs the CA based on a multiple random seeds model in conjunction with a land-use cost matrix, neighborhood weights, and scenario-based land-use quantity for a comprehensive analysis to ultimately facilitate the allocation and simulate spatial distribution for each land type. In our study, the PLUS model was utilized to analyze the driving forces of landscape changes in the Shengjin Lake Reserve and to simulate the landscape distribution under different development scenarios.

2.3.3. Accuracy Assessment of PLUS Model

To assess the accuracy of the PLUS model in simulating the landscape of lacustrine wetlands, we selected landscape classification images and eight driving factors in 2015 and used the PLUS model to simulate the landscape distribution of the reserve in 2020. The 2020 landscape classification images were used as the truth landscape for evaluating the simulation accuracy. This study used the kappa coefficient, overall accuracy (OA), and figure of merit (FOM) values to evaluate the simulation accuracy. The specific formulas are as follows:

Kappa Coefficient: this is used to measure classification accuracy.

$$\text{Kappa} = \frac{p_o - p_c}{p_p - p_c} \quad (1)$$

where P_o is the proportion of correctly simulated pixels, P_p is the proportion of correctly predicted pixels in an ideal situation, and P_c is the proportion of correctly predicted pixels in a random situation. The closer the kappa coefficient is to 1, the better the classification result matches the actual situation.

Overall accuracy (OA): this is used to measure the prediction accuracy of the model and is the ratio of the correctly classified samples to the total number of samples.

$$OA = \frac{\sum_{i=1}^n X_{ii}}{N} \quad (2)$$

where X_{ii} represents the number of correctly classified samples along the diagonal, and N is the total number of samples. The higher the OA value, the better the overall prediction accuracy of the model.

Figure of merit (FOM): this is a less commonly used accuracy evaluation metric, typically applied in change detection to measure the model's prediction accuracy in areas of change [45].

$$FOM = \frac{A_{ij}}{A_{ij} + B + C + D} \quad (3)$$

where A_{ij} is the area correctly predicted as a change, B is the area incorrectly predicted as a change, C is the area incorrectly predicted as no change, and D is the area where no actual change occurred. The closer the FOM value is to 1, the higher the prediction accuracy in the change areas.

Additionally, landscape classification data from 2010, 2015, and 2020 were used to generate development probability maps of various landscape types at different intervals using the PLUS model's LEAS (Figure S1). Comparative experiments were conducted by setting different initial years, time intervals, and driving factors to simulate the landscape distribution of the reserve in 2020. The 2020 remote sensing classification image was used as validation data, and the kappa coefficient, OA, and FOM values were utilized to explore the applicability of the PLUS model in simulating the Lacustrine wetlands landscape.

2.3.4. Different Development Scenario Settings

To explore the future trends of landscape pattern in Shengjin Lake Reserve under different scenarios, we established natural development, urban development, and ecological protection scenarios based on previous research [22,46,47] and used a land-use conversion cost matrix for each scenario to predict the landscape distribution in 2030 (Table 4). In the natural development scenario, most landscape type conversions were unrestricted; however, based on the actual conditions and the limitations of remote sensing interpretation, certain conversions between landscape types were reasonably restricted. For instance, field surveys and long-term monitoring data revealed that conversions between grass beach and built-up land rarely occur in the short term, so these specific conversions were restricted in the transfer matrix (marked as 0). These restrictions, grounded in actual geographic and ecological conditions, ensure that the model’s simulation results align more closely with reality, while the conversion probabilities between other landscape types remained unchanged; in the urban development scenario, the conversion of built-up land to other categories was restricted, and the probability of cropland, woodland, and reservoir/pond turning into built-up land increased by 20% (Table S1); and in the ecological protection scenario, the conversion of grass beach to landscapes other than mudflats and lakes is restricted, while woodland can only be converted to itself or to lakes. Additionally, the conversion probabilities for ecological land were also adjusted, and the probability of converting other landscapes to built-up land and reservoirs/ponds was reduced by 30% (Table S1). Due to the unavailability of the central lake in the reserve, it was set as constrained regions in all scenarios.

Table 4. Land-use conversion cost matrix for different development scenarios.

Scenario Settings	Natural Development Scenario (NDS)							Urban Development Scenario (UDS)							Ecological Protection Scenario (EPS)						
	a	b	c	d	e	f	g	a	b	c	d	e	f	g	a	b	c	d	e	f	g
a	1	1	0	1	1	1	1	1	1	0	1	1	1	1	1	0	0	0	0	1	1
b	1	1	1	1	1	1	0	1	1	1	1	1	1	1	1	1	1	1	1	1	1
c	0	1	1	1	1	1	0	0	0	1	0	0	0	0	0	1	1	1	1	1	1
d	1	1	1	1	1	1	1	1	1	1	1	1	1	1	0	0	0	1	0	0	1
e	0	1	1	1	1	1	1	0	1	1	1	1	1	1	0	1	1	1	1	1	1
f	1	1	1	1	1	1	1	1	1	1	1	1	1	1	1	0	0	0	1	1	1
g	1	1	1	1	1	1	1	1	1	0	1	1	1	1	1	0	0	0	0	1	1

Note: a, b, c, d, e, f, and g represent grass beach, cropland, built-up land, woodland, reservoirs/ponds, mudflats, and lakes, respectively; 0 indicates no conversion allowed and 1 indicates conversion allowed; and rows in the matrix denote the source and the columns denote the destination.

3. Results

3.1. Landscape Change During 2010–2020

Figure 2 presents spatial distribution and proportion of landscape types in the Shengjin Lake Reserve from 2010 to 2020. Cropland was the predominant landscape type in the reserve, accounting for more than 30%, and was mainly located in the western and northern parts of the reserve, with a decreasing trend since 2010. Lakes, as the second major landscape type, also exhibited a declining trend. Built-up land was relatively dispersed and had an increasing trend. Concurrently, the proportion of reservoirs/ponds increased, increasing from 3.3% to 7.55%. The natural wetland landscapes (including grass beaches, mudflats, and lakes) did not significantly change over the last decade, yet there was intense interchange among these three landscape types. In particular, the proportion of mudflats significantly increased by 12.03%, directly resulting in a decrease in lakes and grass beaches. Woodland concentrated in the northeastern and southwestern parts of the reserve initially decreased and then increased, with an overall increasing trend.

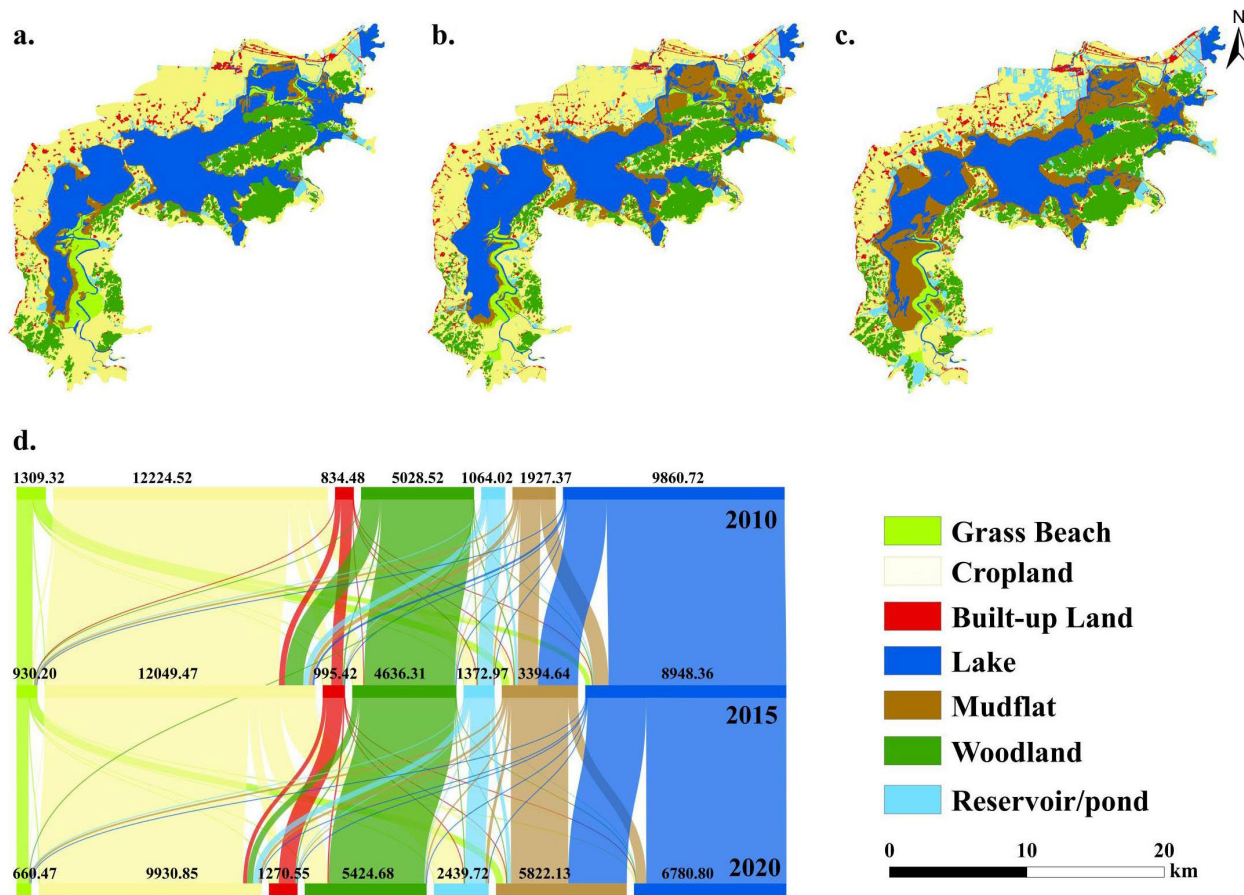


Figure 2. Landscape type distribution of Shengjin Lake Reserve. (a) 2010; (b) 2015; (c) 2020; and (d) landscape area change and transfer of each year.

Table S1 shows the dynamic transitions among landscape types in the reserve from 2010 to 2020. During this period, landscape transitions were primarily between mudflats and lakes, as well as between croplands and reservoirs/ponds. The increase in mudflat area was particularly obvious, which was mainly derived from lakes (75%) and grass beaches (16.69%). Mudflats also served as the main transfer direction for lakes and grass beaches, with a transfer rate from grass beaches to mudflats as high as 88.34%. The area transferred into reservoirs/ponds reached 1710.158 hectares, which was predominantly converted from cropland. Simultaneously, built-up land expanded rapidly and was mainly converted from cropland (80.36%) and woodland (11.04%).

3.2. Landscape Simulation Accuracy of PLUS Model and Driving Force Analysis

3.2.1. Accuracy Evaluation of Landscape Simulation

We evaluated the accuracy of the 2020 landscape simulation using the 2020 landscape classification map (Figure 3a,b). Figure 3 indicates that the kappa coefficient reached 0.8131, the OA value was 0.8516, and the FOM value was 0.3513, showing a relatively consistent distribution. The kappa coefficient was greater than 0.75, which demonstrates that the PLUS model can meet the accuracy requirements of landscape prediction [21]. Due to the complexity of land-use change dynamics, FOM values between 0.2 and 0.4 are also considered acceptable in regional-scale simulations [45]. Thus, the PLUS model is suitable for simulating and predicting lacustrine wetlands landscapes in our study.

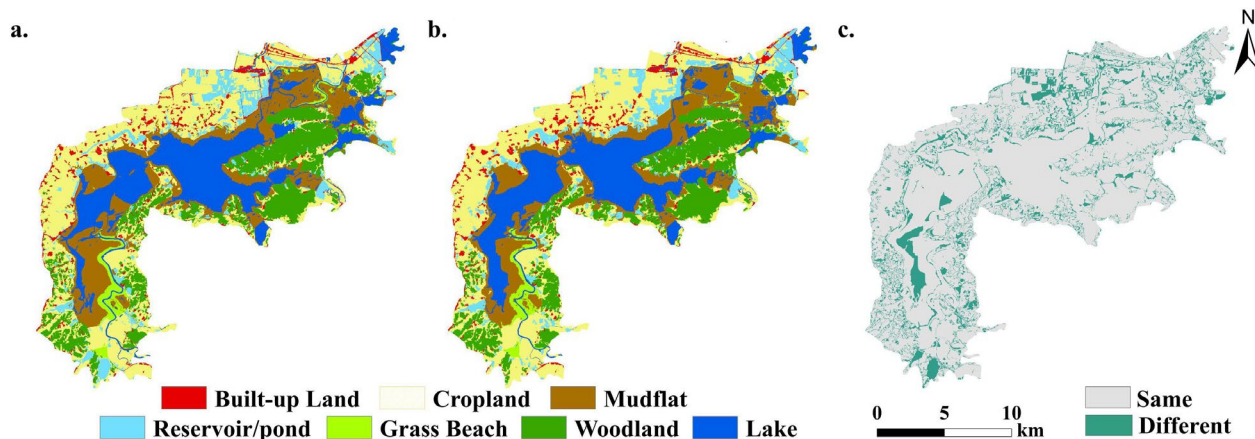


Figure 3. Accuracy assessment of landscape simulation in 2020. (a) Actual landscape in 2020; (b) simulated landscape in 2020; (c) landscape simulation differences.

We further analyzed the spatial differences between the simulated and actual landscapes (Figure 3c). The results show that the simulated landscapes for mudflats and reservoirs/ponds in the northern and southern parts of the reserve differed from the actual distribution. These discrepancies can be attributed to the impacts of regional development policies and socio-economic activities on the reservoir/pond expansion. The PLUS model does not integrate these specific development conditions, limiting its predictive accuracy. Because mudflats are strongly influenced by adjacent lake landscapes, the PLUS model does not consider spatial interactions and may fail to simulate transitions between landscape types. Despite prediction deviations in certain types, such as mudflats and reservoirs/ponds, the overall prediction accuracy of the PLUS model remains high. Accuracy evaluation metrics indicate that the model's overall performance meets the accuracy requirements for wetland landscape prediction. Particularly, the model shows high accuracy in predicting the distribution of most landscape types within the reserve, with relatively consistent spatial distribution.

To evaluate the limiting factor for the simulation accuracy of the PLUS model, we used 2010 and 2015 as the starting years and simulated the 2020 landscape distribution in the reserve using the same landscape development probability parameters with a 5-year interval (Figure 4a,b). The simulation starting in 2015 yielded a kappa coefficient and OA of 0.8031 and 0.8442, respectively, demonstrating higher precision than the simulation starting in 2010, which had a kappa coefficient of 0.7699 and an OA of 0.8105. The simulation results using 2015 as the initial year were closer to the actual landscape. This indicates that the closer the model's input year was to the simulation year, the higher the accuracy of the landscape simulation. Subsequently, we used a 5-year interval based on the period 2015–2020 and a 10-year interval based on the period 2010–2020, with both simulations starting from the same baseline year of 2010 (Figure 5a,b). The results illustrate that the simulations with 5-year intervals yielded a kappa coefficient and OA of 0.8131 and 0.8516, respectively, while the accuracy of the 10-year interval simulations was slightly lower, with a kappa coefficient of 0.7572 and an OA of 0.8132.

To explore the impact of different combinations of driving factors on the simulation accuracy of the PLUS model, we identified combinations of driving factors that showed good accuracy performance. We ranked the driving factors according to their contribution and frequency of occurrence in landscape expansion and established 14 groups of factors to explore their impact on simulation accuracy (Table 5). It shows that the simulation accuracy of the PLUS model varied with the input of driving factors. When removing factors such as slope, GDP, annual average temperature, elevation, and population, although there was a slight decrease in simulation accuracy, the kappa coefficient and OA still remained above 0.8. However, when only the distance to towns, precipitation, and road distance were used as driving factors in Group 10, the accuracy was close to that of Groups 1–6, indicating that

these three factors impacted the simulation accuracy significantly and could be considered as the key driver factors for wetland landscape prediction. Compared to other groups, Group 10 had the simpler combination of factors while still maintaining high simulation accuracy, which enhances the model’s simplicity and interpretability. By focusing on key driving factors contributing substantially to landscape expansion, we can reduce the PLUS model’s complexity while ensuring the operational efficiency and effectiveness in wetland landscape prediction.

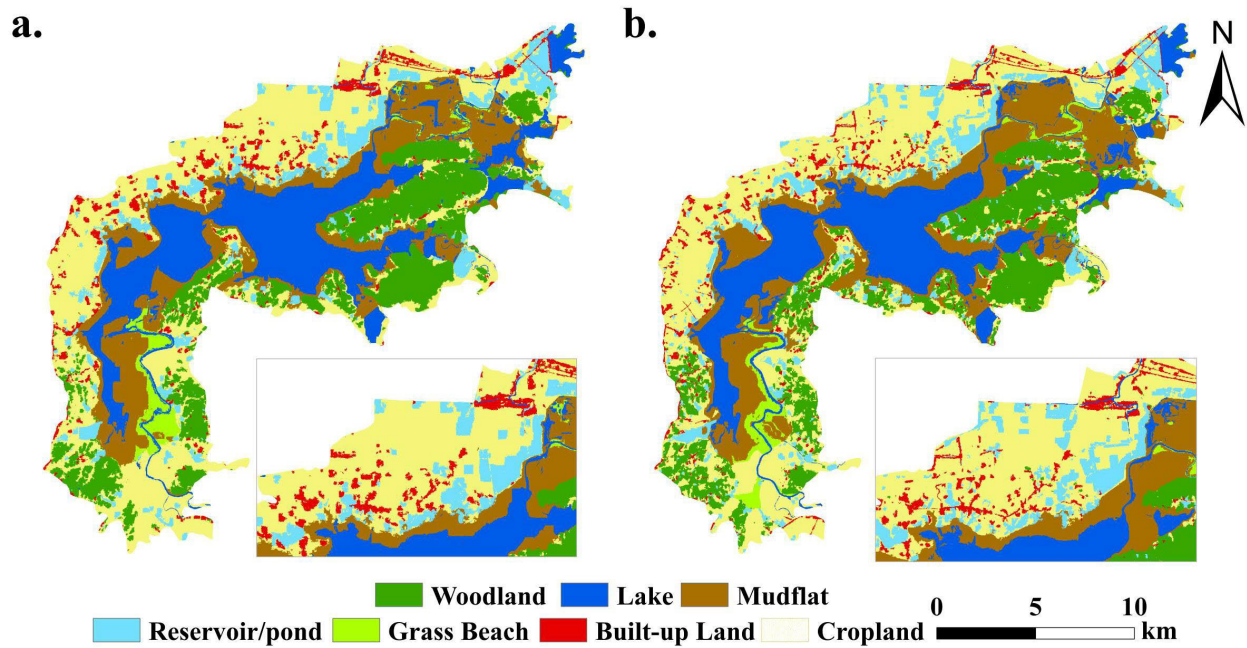


Figure 4. Landscape simulation of the reserve under different initial years. (a) Starting from 2010; (b) starting from 2015.

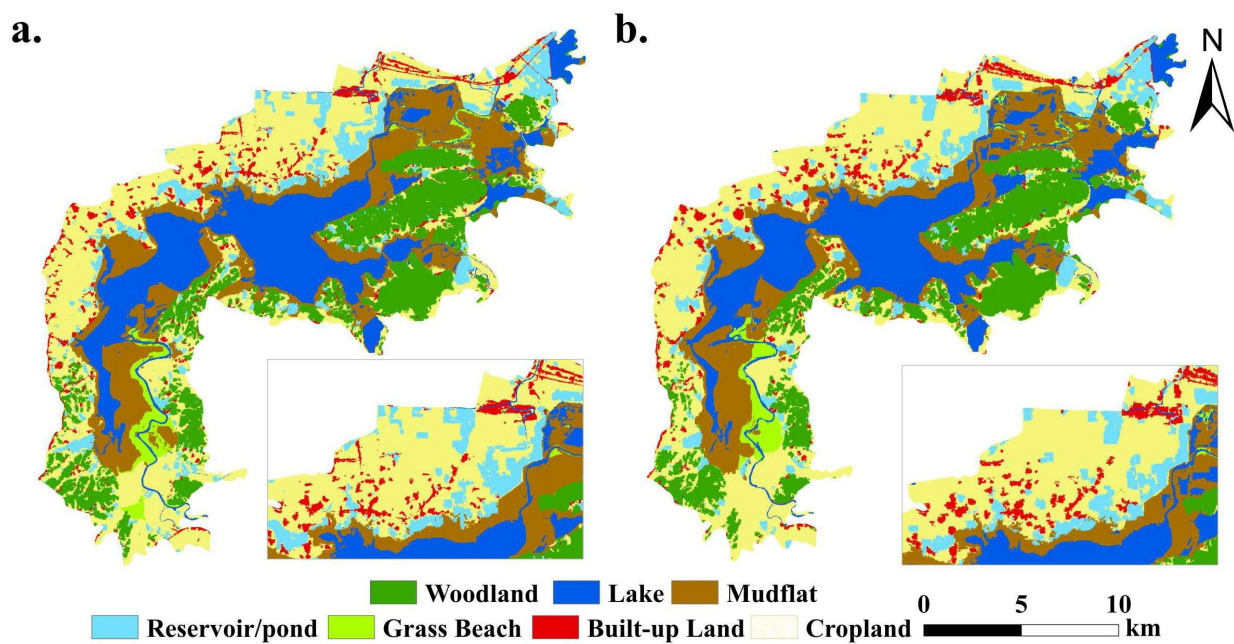


Figure 5. Landscape simulation of the reserve under different time intervals. (a) Five-year interval; (b) ten-year interval.

Table 5. Accuracy assessment of the PLUS model under different combinations of driving factors.

Group	Driving Factors								Kappa Coefficient	Overall Accuracy
1	Dist_road	DEM	PRE	POP	Dist_town	TEM	GDP	Slope	0.81	0.85
2	Dist_road	DEM	PRE	POP	Dist_town	TEM	GDP		0.80	0.84
3	Dist_road	DEM	PRE	POP	Dist_town	TEM			0.80	0.84
4	Dist_road	DEM	PRE	POP	Dist_town				0.80	0.84
5	Dist_road	Dist_town	PRE	POP					0.80	0.84
6	Dist_road	Dist_town	PRE	DEM					0.80	0.84
7	Dist_road	DEM	PRE	POP					0.80	0.84
8	Dist_road	Dist_town	POP	DEM					0.80	0.84
9	Dist_town	DEM	PRE	POP					0.79	0.84
10	Dist_road	Dist_town	PRE						0.80	0.84
11	Dist_road	Dist_town							0.78	0.82
12	Dist_road	PRE							0.77	0.82
13	Dist_town	PRE							0.77	0.82
14	Dist_road								0.68	0.75

Note: POP: population; PRE: precipitation; TEM: temperature; Dist_town: distance from town; Dist_road: distance from road.

3.2.2. Driving Forces of Landscape Change

We calculated the contributions of the driving factors to landscape type expansion in the Shengjin Lake Reserve using the LEAS module of the PLUS model (Figure 6). The figure reveals that the most significant landscape expansion in the reserve occurred in mudflats during 2010–2020, primarily on the northern and southern sides of the lake area, with the main contributing factors of elevation, population, and distance from roads. The primary factors influencing the reservoirs/ponds’ expansion were population, followed by GDP and distance from roads, which are closely linked to human activities, with economic development facilitating the rapid expansion of artificial wetlands. Elevation and distance from roads impacted the expansion of woodlands and croplands significantly. The increase in woodlands may have also been related to the reforestation policies implemented in the reserve since 2017. The primary factors influencing the growth of built-up land were distance from roads, distance from towns, and GDP due to the continuous urbanization process. New built-up land is more likely to be distributed in regions with convenient transportation.

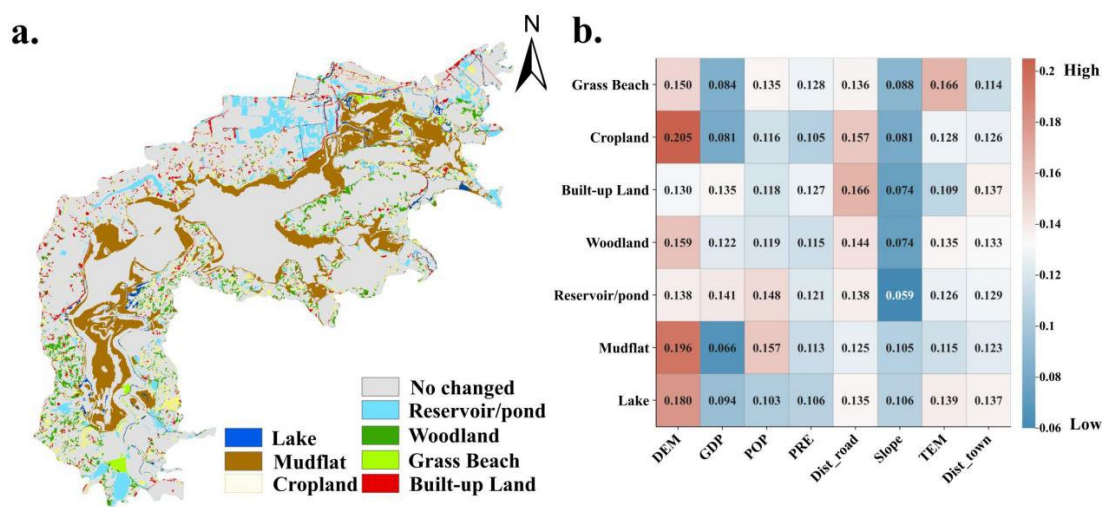


Figure 6. Analysis of the driving forces of landscape changes. (a) Landscape expansion from 2010 to 2020; (b) contribution of driving factors (POP: population; PRE: precipitation; TEM: temperature; Dist_town: distance from town; and Dist_road: distance from road).

3.3. Landscape Prediction Under Different Development Scenarios

Based on the landscape development probabilities and eight driving factors during 2015–2020, with 2020 as the starting year, the PLUS model was used to predict the landscape distribution of the Shengjin Lake Reserve in 2030 under three development scenarios: natural development, urban development, and ecological protection (Figure 7a–c).

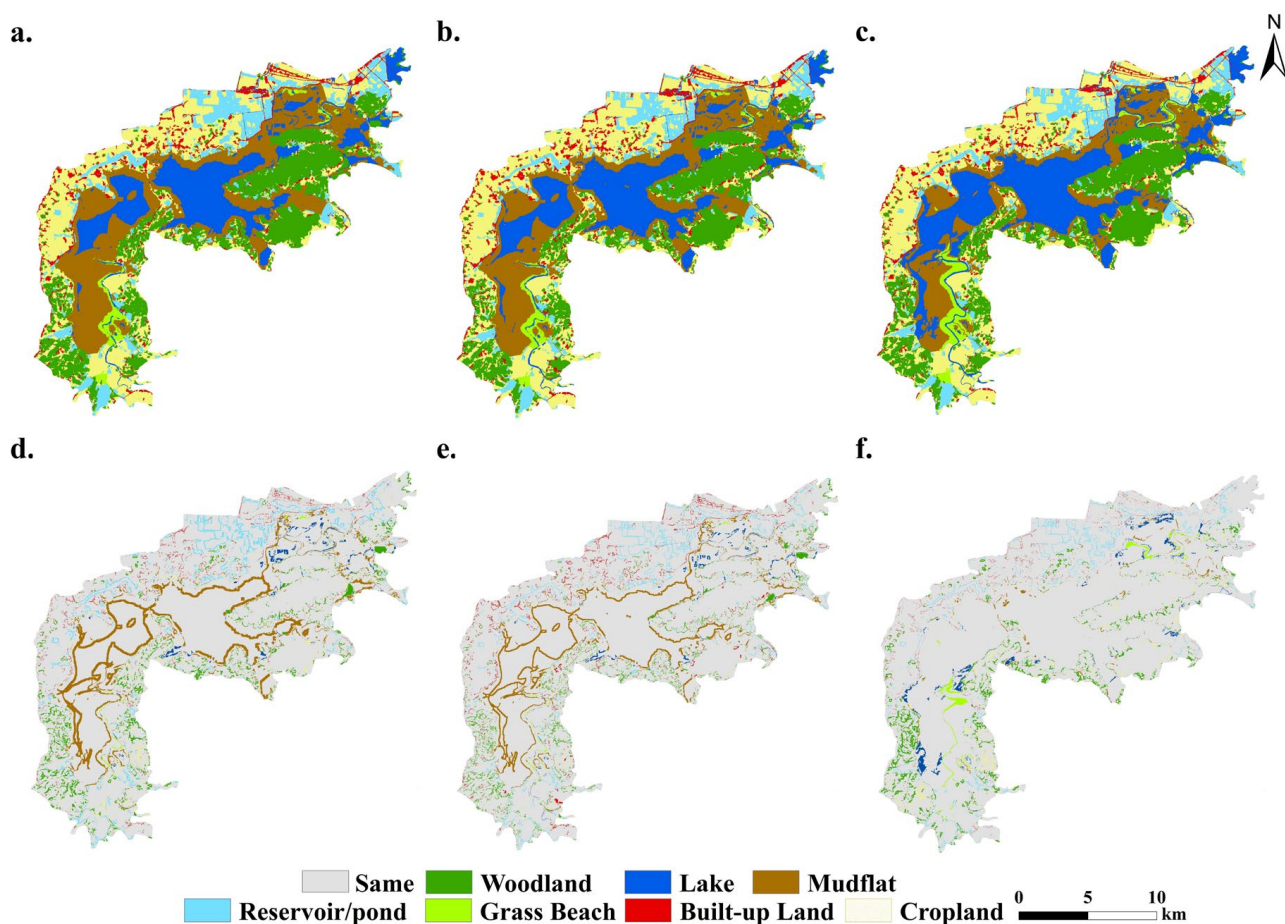


Figure 7. The simulated landscape and landscape expansion in 2030 under different scenarios. (a) NDS; (b) UDS; (c) EPS; and (d–f) landscape expansion in various scenarios compared to 2020.

Under the natural development scenario (Figure 7a,d), compared to those in 2020, the percentages of cropland, grass beaches, and lakes in 2030 will decrease by 6.15%, 0.46%, and 5.27% (Table 6), respectively, while built-up land, woodland, reservoirs/ponds, and mudflats will increase by 0.8%, 2.96%, 2.63%, and 5.49% (Table 6), respectively. Notably, the mudflats' expansion will be the most significant, extending outward along the lake shoreline, indicating the rapid expansion of mudflats without policy intervention, encroaching on other landscape types.

Table 6. Percentage change in landscape area in 2030 under three development scenarios compared to 2020.

	Grass Beach	Cropland	Mudflats	Lake	Built-Up Land	Woodland	Reservoir/Pond
NDS	−0.46%	−6.15%	5.49%	−5.27%	0.80%	2.96%	2.63%
UDS	−0.34%	−4.42%	3.71%	−3.74%	1.36%	1.75%	1.67%
EPS	0.64%	−4.56%	−1.62%	1.05%	0.43%	2.51%	1.56%

Under the urban development scenario (Figure 7b,e), the percentage of built-up land will increase by 1.36%, concentrated in the southern and northern parts of the reserve. Compared to those in the natural development scenario, the decreases in cropland, grass beaches, and lakes reduced, decreasing by 4.42%, 0.34%, and 3.74% (Table 6), respectively. The expansions of woodland, reservoirs/ponds, and mudflats will also decrease to 1.75%, 1.67%, and 3.71%, respectively.

Under the ecological protection scenario (Figure 7c,f), lakes and grass beaches will increase by 1.05% and 0.64% (Table 6), respectively, indicating the effective protection of grass beaches and lakes under this scenario. The expansion of built-up land and reservoirs/ponds will be minimal, increasing by 0.43% and 1.56% (Table 6), respectively. The mudflats proportion will decrease by 1.62%, while that of woodlands will expand by 2.51% (Table 6). Our results show that the ecological protection scenario can effectively guarantee ecological land and plays an important role in maintaining wetland resources in the reserve.

3.4. The Trend of Landscape Pattern Under Different Development Scenarios

Figure S2 shows the landscape indices at the class level of the reserve during 2020–2030 under different development scenarios. Compared to those in 2020, the NP for grass beaches, cropland, mudflats, and lakes in the reserve will increase by 2030, with significant growth in cropland and mudflats. Specifically, under natural and urban development scenarios, the LPIs for cropland and lakes will decrease, while they will increase for other landscapes. Under the ecological protection scenario, both the number and density of lake patches will be lower than those in 2020, indicating the better preservation of lake integrity under this scenario. The decreasing trend of MPS in grass beaches, cropland, and mudflats indicates that these landscapes will become more fragmented. Conversely, the MPS for built-up land, woodland, and reservoirs/ponds will increase, and their landscapes will become more clustered.

Figure S3 illustrates the variations in the landscape indices at the landscape level during 2020–2030 under the three development scenarios. Under the different development scenarios, the landscape indices of the reserve in 2030 exhibited varying trends. The NP value of the reserve will increase, indicating an intensification of landscape fragmentation, most obvious under the natural development scenario. Under the ecological protection scenario, the LSI value is the highest, indicating the most complex landscape shapes and the minimum disturbance of human activities to natural landscapes. The DIVISION values under the three scenarios are 0.938, 0.942, and 0.950, respectively, which are not very different from those in 2020, showing more stable landscape dispersion and resilience. The CONTAG value in the reserve showed a declining trend, indicating reduced landscape connectivity, with the largest reduction under the ecological protection scenario. The increased SHDI and SHEI of the reserve indicates that landscape diversity and internal uniformity will increase under each scenario. Among them, the ecological protection scenario exhibited the highest landscape heterogeneity, indicating that this scenario can effectively enhance landscape diversity and uniformity.

4. Discussion

4.1. Factors Limiting the Accuracy of PLUS Model

Current studies have rarely considered the impact of the initial year and time interval on the simulation accuracy of land-use simulation models [48,49]. The results in this paper confirm that the closer initial year and shorter time interval can effectively improve the landscape simulation accuracy of the PLUS model in lacustrine wetlands. Niu et al. [50] also found that the land-use simulations in the Yangtze River Basin based on 2005–2010 and 2000–2010 were more accurate than those based on 1990–2005, with the lowest accuracy in 15-year interval simulations. This indicates that using longer intervals (15 and 20 years) may reduce the simulation accuracy of the PLUS model, as long time intervals may cause the model to ignore the changes in intermediate years, such as policy shifts, economic activities, or natural disasters, which could be crucial for simulating land-use changes. Therefore,

to enhance the accuracy of landscape simulations, shorter intervals (5 and 10 years) are recommended to better capture the dynamic processes of land-use change [51].

The choice of driving factors is important in determining the landscape simulation accuracy, which can come from natural and socio-economic fields, but their number is often large and fixed [52,53]. Few studies have considered the impact of input driving factors on the simulation accuracy of the PLUS model. Our study demonstrates that the distance from towns, precipitation, and distance from road have significant effects on simulation accuracy in the landscape modeling of Shengjin Lake Wetland Reserve, particularly in a lake wetland area characterized by clear interactions between natural and human activities. These factors are more directly reflective of the driving forces behind changes in lake wetlands within this specific environment. Existing research has indicated that changes in precipitation can affect wetland landscape changes significantly and may exert pressure on surface water levels [20]. Du [54] also proposed that precipitation is one of the main influencing factors for the wetland evolution in the Lesser Khingan Mountains. Furthermore, as human activities such as village construction and road expansion intensify, the distance from towns and roads greatly affects the landscape development probability and the simulation accuracy, consistent with the previous findings [55,56]. These results highlight the importance of these factors in the lacustrine wetlands landscape simulation.

4.2. Influencing Factors of Wetland Landscape Evolution in the Reserve

Wetland landscape evolution is influenced by both natural factors and human activities. In terms of natural factors, previous studies indicated that wetland hydrological conditions, particularly water level fluctuations, have a significant impact on seasonally sensitive lakes, grass beaches, and mudflats [57], which aligns with the findings of our study. The rapid expansion of mudflats in the Shengjin Lake Reserve primarily occurred on the northern and southern sides of the lake, highly sensitive to wetland hydrological conditions. Wetland hydrological processes are influenced by natural factors such as DEM, precipitation, and air temperature. Additionally, long-term agricultural activities have had a significant impact on the expansion of mudflats, as the dense distribution of farmlands around the lake led to soil erosion, resulting in sedimentation in the mudflats [37]. As for human factors, rapid socio-economic development has driven the expansion of built-up land [58], which has also been confirmed in this study. Our study shows that the expansion of built-up land and reservoirs/ponds in the northern part of the reserve is most significant, driven by the factors of population density and distance from towns and roads, which facilitated the expansion of artificial wetlands and built-up land. Furthermore, policies of returning farmland to forests implemented by the reserve after 2017 have also played a positive role in forest land expansion. Overall, natural factors such as water level fluctuation and elevation play a key role in the changes in mudflats and grass beaches, while socio-economic development and policy guidance have influenced the expansion and contraction of artificial wetlands. Ecological protection policies play a positive role in mitigating wetland degradation, further confirming the conclusions of An et al. [20].

Local policy guidance, especially regarding wetland protection and ecological restoration, is still a critical factor in determining the evolution of wetland landscapes [47,59]. This study explores the potential impact of future local policy orientations on the landscape of Shengjin Lake Reserve by setting three different development scenarios. Under the natural development scenario, with no policy intervention, the landscape pattern of the reserve shows an increasing trend of fragmentation. Previous studies indicated that economic development usually has a negative impact on wetland landscape [21,22]. In the urban development scenario driven by economic growth, the continuous reduction in lakes, grass beaches, and cropland in Shengjin Lake Reserve exacerbates landscape fragmentation, further affecting wetland landscapes negatively. In the ecological protection scenario, grass beaches and lakes rarely transform to other landscape types, and the landscape heterogeneity is enhanced, providing maximum protection for the wetland resources of the reserve

and preserving wetland ecosystem services, consistent with the conclusions of the existing research [46,47].

Based on the comprehensive analysis of the future landscape trends in the Shengjin Lake Reserve under different scenarios, the following development recommendations are proposed: (1) The ecological protection scenario is suitable as a future development strategy for the reserve as it can protect the ecological space of natural wetland resources effectively. However, cropland will continue to decrease under this scenario, and the red line of cropland protection should be strictly observed in the future [57]. (2) The connectivity between wetland landscape patches should be enhanced, and the aggregation of ecological space should be strengthened to maintain the stability of wetland landscapes [60]. (3) Due to the intense transitions among grass beaches, mudflats, and lakes, enhancing their hydrological connectivity can optimize the landscape pattern and fully utilize the ecosystem service of wetlands [61].

4.3. Innovations, Limitations, and Future Perspectives

Based on the landscape dynamic analysis of Shengjin Lake Reserve from 2010 to 2020, we explore the applicability and limiting factors of the PLUS model in the simulation of the lacustrine wetlands landscape and explore the evolution trend of wetland landscapes under different development scenarios according to the prediction landscape results of future years, which are also the main innovations of this study. Regarding the accuracy of the wetland landscape simulation, this study uses remote sensing interpretation data as the real landscape data to validate the applicability of the PLUS model. The influence of the initial year selection, the setting of the time interval, and the selection of a driver factor on the simulation accuracy of the model were also analyzed by setting different input conditions, which are often ignored in previous studies of the wetland landscape simulation.

This study also has some limitations. Although the PLUS model can simulate the spatial pattern of wetland landscape effectively, it still needs to be improved in handling the interaction and feedback mechanism among landscape types. In particular, the interaction between the wetland landscape and hydrological processes is relatively complex, and the model fails to consider the effects of hydrological connectivity and water level fluctuations on the wetland landscape dynamics. Moreover, some important human driving factors (e.g., policy guidance and human activities) could not be included in the model due to a lack of data, which may lead to limitations on the accuracy of future scenario predictions.

In future research, high-resolution remote sensing images and hydrological models [62] could be further coupled to enhance the PLUS model's capacity to simulate wetland hydrological processes and improve the accuracy of the wetland landscape simulation. Additionally, as climate change intensifies, the role of climate factors in the evolution of wetland landscapes will become more important. Therefore, the combination of a climate model [63] and landscape simulation should be further strengthened to explore the evolution trend of wetland landscapes under different climate scenarios in the future.

5. Conclusions

This study utilized remote sensing images to analyze the dynamic characteristics of wetland landscapes in Shengjin Lake Reserve from 2010 to 2020. Based on this, the PLUS model was employed to simulate wetland landscapes, investigating the model's accuracy and limitations in simulating lacustrine wetlands and predicting the future trends in wetland landscapes under different development scenarios. The results indicate that the dominant landscape types in the reserve are cropland and lakes, accounting for more than 50%. During 2010–2020, cropland, lakes, and grass beaches decreased, while built-up land, reservoirs/ponds, and mudflats increased, with woodland initially decreasing and then increasing, leading to an increasingly fragmented landscape pattern. The applicability of the PLUS model for simulating lacustrine wetlands landscapes is satisfactory, with the OA value exceeding 80%, kappa coefficient value above 0.75, and FOM value of 0.35. The simulation accuracy of the PLUS model can be improved effectively by selecting the

input parameters such as closer initial year, shorter time interval, and key drivers. The evolutionary trends of wetland landscapes are quite different under different development scenarios. Under the natural development scenario, grass beach, cropland, and lake are reduced, while mudflats expand significantly; under the urban development scenario, built-up land grows rapidly, while grass beach, lake, and cropland decrease; and under the ecological protection scenario, the growth of grass beach, lakes, and woodland is more noticeable, the mudflats shrink, landscape shapes become more complex, and landscape heterogeneity is enhanced, which guarantees ecological land effectively. Therefore, we recommended the adoption of an ecological conservation development strategy as the future policy orientation for the reserve.

Supplementary Materials: The following supporting information can be downloaded at: <https://www.mdpi.com/article/10.3390/rs16224169/s1>, Figure S1: Probability of landscape change at different intervals; Figure S2: Variations in landscape indices at the class level in the reserve from 2010 to 2030; Figure S3: Variations in landscape indices at the landscape level during 2010–2030 under different scenarios; Table S1: Landscape development probability under different scenarios; Table S2: Landscape Transition Matrix of the Reserve during 2010–2020.

Author Contributions: Conceptualization, Z.Z. and J.W.; methodology, Z.Z.; software, Z.Z.; validation, Z.Z.; formal analysis, Z.Z.; data curation, Z.Z.; writing—original draft, Z.Z.; project administration, J.W.; writing—review and editing, J.W., Y.C. and J.N.; supervision, J.W., Y.C. and J.N.; investigation, Q.Z. All authors have read and agreed to the published version of the manuscript.

Funding: This research was supported by the National Natural Science Foundation of China, grant number “32171573”, Anhui Provincial Natural Science Foundation, grant number “2308085MD114, 2308085Y29”, and the Key Research and Development Project of Anhui Province, grant number “2022107020027”.

Data Availability Statement: The original contributions presented in the study are included in the article/Supplementary Materials, further inquiries can be directed to the corresponding author/s.

Conflicts of Interest: The authors declare no conflicts of interest.

References

1. Qin, L.; Jiang, M.; Freeman, C.; Zou, Y.; Gao, C.; Tian, W.; Wang, G. Agricultural Land Use Regulates the Fate of Soil Phosphorus Fractions Following the Reclamation of Wetlands. *Sci. Total Environ.* **2023**, *863*, 160891. [[CrossRef](#)] [[PubMed](#)]
2. Narayan, S.; Beck, M.W.; Wilson, P.; Thomas, C.J.; Guerrero, A.; Shepard, C.C.; Reguero, B.G.; Franco, G.; Ingram, J.C.; Trespalacios, D. The Value of Coastal Wetlands for Flood Damage Reduction in the Northeastern USA. *Sci. Rep.* **2017**, *7*, 9463. [[CrossRef](#)] [[PubMed](#)]
3. Mitsch, W.J.; Bernal, B.; Nahlik, A.M.; Mander, U.; Zhang, L.; Anderson, C.J.; Jorgensen, S.E.; Brix, H. Wetlands, Carbon, and Climate Change. *Landsc. Ecol.* **2013**, *28*, 583–597. [[CrossRef](#)]
4. Song, F.; Su, F.; Mi, C.; Sun, D. Analysis of Driving Forces on Wetland Ecosystem Services Value Change: A Case in Northeast China. *Sci. Total Environ.* **2021**, *751*, 141778. [[CrossRef](#)]
5. Dadashpoor, H.; Azizi, P.; Moghadasi, M. Land Use Change, Urbanization, and Change in Landscape Pattern in a Metropolitan Area. *Sci. Total Environ.* **2019**, *655*, 707–719. [[CrossRef](#)] [[PubMed](#)]
6. Zhang, M.; Gong, Z.; Zhao, W.; Duo, A. Landscape pattern change and the driving forces in Baiyangdian wetland from 1984 to 2014. *Acta Ecol. Sin.* **2016**, *36*, 4780–4791.
7. Lv, J.; Jiang, W.; Wang, W.; Chen, K.; Deng, Y.; Chen, Z.; Li, Z. Wetland landscape pattern change and its driving forces in Beijing-Tianjin-Hebei region in recent 30 years. *Acta Ecol. Sin.* **2018**, *38*, 4492–4503.
8. Luo, G.; Amuti, T.; Zhu, L.; Mambetov, B.T.; Maisupova, B.; Zhang, C. Dynamics of Landscape Patterns in an Inland River Delta of Central Asia Based on a Cellular Automata-Markov Model. *Reg. Environ. Chang.* **2015**, *15*, 277–289. [[CrossRef](#)]
9. Wang, P.; Li, R.; Liu, D.; Wu, Y. Dynamic Characteristics and Responses of Ecosystem Services under Land Use/Land Cover Change Scenarios in the Huangshui River Basin, China. *Ecol. Indic.* **2022**, *144*, 109539. [[CrossRef](#)]
10. Fu, F.; Deng, S.; Wu, D.; Liu, W.; Bai, Z. Research on the Spatiotemporal Evolution of Land Use Landscape Pattern in a County Area Based on CA-Markov Model. *Sustain. Cities Soc.* **2022**, *80*, 103760. [[CrossRef](#)]
11. Liao, G.; He, P.; Gao, X.; Lin, Z.; Huang, C.; Zhou, W.; Deng, O.; Xu, C.; Deng, L. Land Use Optimization of Rural Production-Living-Ecological Space at Different Scales Based on the BP-ANN and CLUE-S Models. *Ecol. Indic.* **2022**, *137*, 108710. [[CrossRef](#)]
12. Lukas, P.; Melesse, A.M.; Kenea, T.T. Prediction of Future Land Use/Land Cover Changes Using a Coupled CA-ANN Model in the Upper Omo-Gibe River Basin, Ethiopia. *Remote Sens.* **2023**, *15*, 1148. [[CrossRef](#)]

13. Liu, X.; Liang, X.; Li, X.; Xu, X.; Ou, J.; Chen, Y.; Li, S.; Wang, S.; Pei, F. A Future Land Use Simulation Model (FLUS) for Simulating Multiple Land Use Scenarios by Coupling Human and Natural Effects. *Landsc. Urban Plan.* **2017**, *168*, 94–116. [[CrossRef](#)]
14. Li, X.; Liu, X.; Lao, C.; Zhang, Y.; He, J.; Huang, K. The implementation and application of geographical simulation and optimization systems (GeoSOS). *Acta Sci. Nat. Univ.* **2010**, *49*, 1–5.
15. Qian, Y.; Xing, W.; Guan, X.; Yang, T.; Wu, H. Coupling Cellular Automata with Area Partitioning and Spatiotemporal Convolution for Dynamic Land Use Change Simulation. *Sci. Total Environ.* **2020**, *722*, 137738. [[CrossRef](#)]
16. Li, S.; Liu, X.; Li, X.; Chen, Y. Simulation model of land use dynamics and application: Progress and prospects. *J. Remote Sens.* **2017**, *21*, 329–340. [[CrossRef](#)]
17. Ren, Y.; Lu, Y.; Comber, A.; Fu, B.; Harris, P.; Wu, L. Spatially Explicit Simulation of Land Use/Land Cover Changes: Current Coverage and Future Prospects. *Earth-Sci. Rev.* **2019**, *190*, 398–415. [[CrossRef](#)]
18. Xu, L.; Liu, X.; Tong, D.; Liu, Z.; Yin, L.; Zheng, W. Forecasting Urban Land Use Change Based on Cellular Automata and the PLUS Model. *Land* **2022**, *11*, 652. [[CrossRef](#)]
19. Wang, Z.; Gao, Y.; Wang, X.; Lin, Q.; Li, L. A New Approach to Land Use Optimization and Simulation Considering Urban Development Sustainability: A Case Study of Bortala, China. *Sustain. Cities Soc.* **2022**, *87*, 104135. [[CrossRef](#)]
20. An, X.; Zhang, M.; Zang, Z. Driving Mechanisms of Spatiotemporal Heterogeneity of Land Use Conflicts and Simulation under Multiple Scenarios in Dongting Lake Area. *Remote Sens.* **2023**, *15*, 4524. [[CrossRef](#)]
21. Zhang, S.; Zhong, Q.; Cheng, D.; Xu, C.; Chang, Y.; Lin, Y.; Li, B. Landscape Ecological Risk Projection Based on the PLUS Model under the Localized Shared Socioeconomic Pathways in the Fujian Delta Region. *Ecol. Indic.* **2022**, *136*, 108642. [[CrossRef](#)]
22. Wang, Q.; Guan, Q.; Sun, Y.; Du, Q.; Xiao, X.; Luo, H.; Zhang, J.; Mi, J. Simulation of Future Land Use/Cover Change (LUCC) in Typical Watersheds of Arid Regions under Multiple Scenarios. *J. Environ. Manag.* **2023**, *335*, 117543. [[CrossRef](#)]
23. Cai, G.; Lin, Y.; Zhang, F.; Zhang, S.; Wen, L.; Li, B. Response of Ecosystem Service Value to Landscape Pattern Changes under Low-Carbon Scenario: A Case Study of Fujian Coastal Areas. *Land* **2022**, *11*, 2333. [[CrossRef](#)]
24. Bao, R.; Alonso, A.; Delgado, C.; Pages, J.L. Identification of the Main Driving Mechanisms in the Evolution of a Small Coastal Wetland (Traba, Galicia, NW Spain) since Its Origin 5700 Cal Yr BP. *Paleogeogr. Paleoclimatol. Paleoecol.* **2007**, *247*, 296–312. [[CrossRef](#)]
25. Serra, P.; Pons, X.; Sauri, D. Land-Cover and Land-Use Change in a Mediterranean Landscape: A Spatial Analysis of Driving Forces Integrating Biophysical and Human Factors. *Appl. Geogr.* **2008**, *28*, 189–209. [[CrossRef](#)]
26. Hu, X.; Xu, W.; Li, F. Spatiotemporal Evolution and Optimization of Landscape Patterns Based on the Ecological Restoration of Territorial Space. *Land* **2022**, *11*, 2114. [[CrossRef](#)]
27. Cao, M.; Tang, G.; Shen, Q.; Wang, Y. A New Discovery of Transition Rules for Cellular Automata by Using Cuckoo Search Algorithm. *Int. J. Geogr. Inf. Sci.* **2015**, *29*, 806–824. [[CrossRef](#)]
28. Omrani, H.; Parmentier, B.; Helbich, M.; Pijanowski, B. The Land Transformation Model-Cluster Framework: Applying *k*-Means and the Spark Computing Environment for Large Scale Land Change Analytics. *Environ. Model. Softw.* **2019**, *111*, 182–191. [[CrossRef](#)]
29. Meentemeyer, R.K.; Tang, W.; Durning, M.A.; Vogler, J.B.; Cunniffe, N.J.; Shoemaker, D.A. FUTURES: Multilevel Simulations of Emerging Urban-Rural Landscape Structure Using a Stochastic Patch-Growing Algorithm. *Ann. Assoc. Am. Geogr.* **2013**, *103*, 785–807. [[CrossRef](#)]
30. Liang, X.; Guan, Q.; Clarke, K.C.; Liu, S.; Wang, B.; Yao, Y. Understanding the Drivers of Sustainable Land Expansion Using a Patch-Generating Land Use Simulation (PLUS) Model: A Case Study in Wuhan, China. *Comput. Environ. Urban Syst.* **2021**, *85*, 101569. [[CrossRef](#)]
31. Li, Y.; Geng, H. Evolution of Land Use Landscape Patterns in Karst Watersheds of Guizhou Plateau and Its Ecological Security Evaluation. *Land* **2022**, *11*, 2225. [[CrossRef](#)]
32. Cui, Y.; Dong, B.; Chen, L.; Gao, X.; Cui, Y. Study on Habitat Suitability of Overwintering Cranes Based on Landscape Pattern Change: A Case Study of Typical Lake Wetlands in the Middle and Lower Reaches of the Yangtze River. *Environ. Sci. Pollut. Res.* **2019**, *26*, 14976. [[CrossRef](#)] [[PubMed](#)]
33. Xie, C.; Dai, B.; Wu, J.; Liu, Y.; Jiang, Z. Initial Recovery of Fish Faunas Following the Implementation of Pen-Culture and Fishing Bans in Floodplain Lakes along the Yangtze River. *J. Environ. Manag.* **2022**, *319*, 115743. [[CrossRef](#)] [[PubMed](#)]
34. Zhou, J.; Zhou, L.; Xu, W. Diversity of Wintering Waterbirds Enhanced by Restoring Aquatic Vegetation at Shengjin Lake, China. *Sci. Total Environ.* **2020**, *737*, 140190. [[CrossRef](#)] [[PubMed](#)]
35. Song, Y.; Zhou, L. Effects of habitat changes on spatio-temporal pattern of the wintering waterbird community at Shengjin Lake. *J. Anhui Agric. Univ.* **2019**, *46*, 610–617. [[CrossRef](#)]
36. Li, S.; Dong, B.; Gao, X.; Wang, P.; Ye, X.K.; Xu, H.; Ren, C. Land Use Change and Driving Forces in Shengjin Lake Wetland in Anhui Province, China. *J. Appl. Remote Sens.* **2021**, *15*, 042404. [[CrossRef](#)]
37. Zhang, Y.; Wang, D.; Zhou, Q. Landscape Pattern Change of Shengjin Lake Wetland from 1993 to 2016 and Its Response to Human Disturbance. In Proceedings of the 2019 8th International Conference on Agro-Geoinformatics (Agro-Geoinformatics), Istanbul, Turkey, 16–19 July 2019; IEEE: New York, NY, USA, 2019.
38. Wu, P.; Zhan, W.; Cheng, N.; Yang, H.; Wu, Y. A Framework to Calculate Annual Landscape Ecological Risk Index Based on Land Use/Land Cover Changes: A Case Study on Shengjin Lake Wetland. *IEEE J. Sel. Top. Appl. Earth Observ. Remote Sens.* **2021**, *14*, 11926–11935. [[CrossRef](#)]

39. GB/T 21010-2017; Classification of Land Use Status. China National Standardization Administration: Beijing, China, 2017.
40. Mao, D.; Wang, Z.; Du, B.; Li, L.; Tian, Y.; Jia, M.; Zeng, Y.; Song, K.; Jiang, M.; Wang, Y. National Wetland Mapping in China: A New Product Resulting from Object-Based and Hierarchical Classification of Landsat 8 OLI Images. *ISPRS J. Photogramm. Remote Sens.* **2020**, *164*, 11–25. [[CrossRef](#)]
41. Mahdavi, S.; Salehi, B.; Granger, J.; Amani, M.; Brisco, B.; Huang, W. Remote Sensing for Wetland Classification: A Comprehensive Review. *GISci. Remote Sens.* **2018**, *55*, 623–658. [[CrossRef](#)]
42. Fan, C.; Myint, S. A Comparison of Spatial Autocorrelation Indices and Landscape Metrics in Measuring Urban Landscape Fragmentation. *Landsc. Urban Plan.* **2014**, *121*, 117–128. [[CrossRef](#)]
43. Wang, H.; Zhang, M.; Wang, C.; Wang, K.; Wang, C.; Li, Y.; Bai, X.; Zhou, Y. Spatial and Temporal Changes of Landscape Patterns and Their Effects on Ecosystem Services in the Huaihe River Basin, China. *Land* **2022**, *11*, 513. [[CrossRef](#)]
44. Wang, S.; Zuo, Q.; Zhou, K.; Wang, J.; Wang, W. Predictions of Land Use/Land Cover Change and Landscape Pattern Analysis in the Lower Reaches of the Tarim River, China. *Land* **2023**, *12*, 1093. [[CrossRef](#)]
45. Pontius, R.G.; Millones, M. Death to Kappa: Birth of Quantity Disagreement and Allocation Disagreement for Accuracy Assessment. *Int. J. Remote Sens.* **2011**, *32*, 4407–4429. [[CrossRef](#)]
46. Li, C.; Wu, Y.; Gao, B.; Zheng, K.; Wu, Y.; Li, C. Multi-Scenario Simulation of Ecosystem Service Value for Optimization of Land Use in the Sichuan-Yunnan Ecological Barrier, China. *Ecol. Indic.* **2021**, *132*, 108328. [[CrossRef](#)]
47. Nie, W.; Xu, B.; Yang, F.; Shi, Y.; Liu, B.; Wu, R.; Lin, W.; Pei, H.; Bao, Z. Simulating Future Land Use by Coupling Ecological Security Patterns and Multiple Scenarios. *Sci. Total Environ.* **2023**, *859*, 160262. [[CrossRef](#)]
48. Li, X.; Fu, J.; Jiang, D.; Lin, G.; Cao, C. Land Use Optimization in Ningbo City with a Coupled GA and PLUS Model. *J. Clean Prod.* **2022**, *375*, 134004. [[CrossRef](#)]
49. Gao, L.; Tao, F.; Liu, R.; Wang, Z.; Leng, H.; Zhou, T. Multi-Scenario Simulation and Ecological Risk Analysis of Land Use Based on the PLUS Model: A Case Study of Nanjing. *Sustain. Cities Soc.* **2022**, *85*, 104055. [[CrossRef](#)]
50. Niu, T.; Xiong, L.; Chen, J.; Zhou, Y.; Yin, J.; Liu, D. Land use simulation and multi-scenario prediction of the Yangtze River Basin based on PLUS model. *Eng. J. Wuhan Univ.* **2024**, *57*, 1–16.
51. Yu, B.; Zang, Y.; Wu, C.; Zhao, Z. Spatiotemporal Dynamics of Wetlands and Their Future Multi-Scenario Simulation in the Yellow River Delta, China. *J. Environ. Manag.* **2024**, *353*, 120193. [[CrossRef](#)]
52. Zhang, S.; Yang, P.; Xia, J.; Wang, W.; Cai, W.; Chen, N.; Hu, S.; Luo, X.; Li, J.; Zhan, C. Land Use/Land Cover Prediction and Analysis of the Middle Reaches of the Yangtze River under Different Scenarios. *Sci. Total Environ.* **2022**, *833*, 155238. [[CrossRef](#)]
53. Zhai, H.; Lv, C.; Liu, W.; Yang, C.; Fan, D.; Wang, Z.; Guan, Q. Understanding Spatio-Temporal Patterns of Land Use/Land Cover Change under Urbanization in Wuhan, China, 2000–2019. *Remote Sens.* **2021**, *13*, 3331. [[CrossRef](#)]
54. Du, Y. The Research on the Dynamic Simulation of Landscape Evolution of Wetland in Xiaoxinganlin. Ph.D. Thesis, Harbin Normal University, Harbin, China, 2021.
55. Zhang, Z.; Hu, B.; Jiang, W.; Qiu, H. Identification and Scenario Prediction of Degree of Wetland Damage in Guangxi Based on the CA-Markov Model. *Ecol. Indic.* **2021**, *127*, 107764. [[CrossRef](#)]
56. Lin, S.; Wang, F. Simulation and analysis of land use scenarios in Guangzhou based on the PLUS model and traffic planning scenario. *J. Agric. Resour. Environ.* **2023**, *40*, 557–569. [[CrossRef](#)]
57. Xu, M.; Niu, L.; Wang, X.; Zhang, Z. Evolution of Farmland Landscape Fragmentation and Its Driving Factors in the Beijing-Tianjin-Hebei Region. *J. Clean. Prod.* **2023**, *418*, 138031. [[CrossRef](#)]
58. Li, J.; Zhou, K.; Dong, H.; Xie, B. Cultivated Land Change, Driving Forces and Its Impact on Landscape Pattern Changes in the Dongting Lake Basin. *Int. J. Environ. Res. Public Health* **2020**, *17*, 7988. [[CrossRef](#)]
59. Jiang, W.; Zhang, Z.; Ling, Z.; Deng, Y. Experience and Future Research Trends of Wetland Protection and Restoration in China. *J. Geogr. Sci.* **2024**, *34*, 229–251. [[CrossRef](#)]
60. Zheng, L.; Wang, Y.; Li, J. Quantifying the Spatial Impact of Landscape Fragmentation on Habitat Quality: A Multi-Temporal Dimensional Comparison between the Yangtze River Economic Belt and Yellow River Basin of China. *Land Use Policy* **2023**, *125*, 106463. [[CrossRef](#)]
61. Zhang, M.; Ma, S.; Gong, J.-W.; Chu, L.; Wang, L.-J. A Coupling Effect of Landscape Patterns on the Spatial and Temporal Distribution of Water Ecosystem Services: A Case Study in the Jianghuai Ecological Economic Zone, China. *Ecol. Indic.* **2023**, *151*, 110299. [[CrossRef](#)]
62. Chu, H.-J.; Lin, Y.-P.; Huang, C.-W.; Hsu, C.-Y.; Chen, H.-Y. Modelling the Hydrologic Effects of Dynamic Land-Use Change Using a Distributed Hydrologic Model and a Spatial Land-Use Allocation Model. *Hydrol. Process.* **2010**, *24*, 2538–2554. [[CrossRef](#)]
63. Li, Z.; Fang, H. Impacts of Climate Change on Water Erosion: A Review. *Earth-Sci. Rev.* **2016**, *163*, 94–117. [[CrossRef](#)]

Disclaimer/Publisher’s Note: The statements, opinions and data contained in all publications are solely those of the individual author(s) and contributor(s) and not of MDPI and/or the editor(s). MDPI and/or the editor(s) disclaim responsibility for any injury to people or property resulting from any ideas, methods, instructions or products referred to in the content.